DOI: 10.1161/CIRCGENETICS.112.964452

Proteomic Identification of Matrix Metalloproteinase Substrates in the Human Vasculature

Running title: *Stegemann et al.; MMP substrates in the vasculature*

Christin Stegemann, PhD[1]; Athanasios Didangelos, PhD[1]; Javier Barallobre-Barreiro, PhD[1]; Sarah Langley, PhD[1]; Kaushik Mandal, MD[2]; Marjan Jahangiri, FRCS[3]; Manuel Mayr, MD, PhD[1]

[1]King's BHF Centre, The James Black Centre, King's College London, London, United Kingdom; [2]Division of Cardiac Surgery, The Johns Hopkins University School of Medicine, Baltimore, MD; [3]Dept of Cardiac Surgery, St. George's Healthcare NHS Trust, London, United Kingdom

Correspondence to:

Prof. Manuel Mayr, MD, PhD

King's British Heart Foundation Centre

King's College London

125 Coldharbour Lane

London SE5 9NU, United Kingdom

Tel: +44 (0) 20 7848 5132

Fax: +44 (0) 20 7848 5296

E-mail: manuel.mayr@kcl.ac.uk

Journal Subject Codes: [144] Other arteriosclerosis; [141] Functional genomics; [97] Other Vascular biology

DOI: 10.1161/CIRCGENETICS.112.964452

Abstract:

Background - Matrix metalloproteinases (MMPs) play a key role in cardiovascular disease, in particular aneurysm formation and plaque rupture. Surprisingly little is known about MMP substrates in the vasculature.

Methods and Results - We used a proteomics approach to identify vascular substrates for three MMPs, one of each of the three major classes of MMPs: Human arteries were incubated with MMP-3 (a member of stromelysins), MMP-9 (considered a gelatinase) and MMP-14 (considered a member of the collagenases and of the membrane–bound MMPs). Candidate substrates were identified by mass spectrometry based on 1) increased release from the arterial tissue upon digestion, 2) spectral evidence for proteolytic degradation after gel separation, and 3) identification of non-tryptic cleavage sites. Using this approach, novel candidates were identified, including ECM proteins associated with the basement membrane, elastic fibers (emilin-1) and other extracellular proteins (periostin, tenascin-X). 74 non-tryptic cleavage sites were detected, many of which were shared among different MMPs. The proteomics findings were validated by immunoblotting and by digesting recombinant/purified proteins with exogenous MMPs. As proof-of-principle, results were related to *in vivo* pathology by searching for corresponding degradation products in human aortic tissue with different levels of endogenous MMP-9.

Conclusions - The application of proteomics to identify MMP targets is a new frontier in cardiovascular research. Our current classification of MMPs based on few substrates is an oversimplification of a complex area of biology. This study provides a more comprehensive assessment of potential MMP substrates in the vasculature and represents a valuable resource for future investigations.

Key words: arteries; atherosclerosis; metalloproteinases; MMP; proteomics

DOI: 10.1161/CIRCGENETICS.112.964452

Introduction

Matrix metalloproteinases (MMPs) are endopeptidases that require zinc as a cofactor. Increased MMP activity is thought to be associated with rupture of vulnerable atherosclerotic plaques and aneurysm formation. Excessive expression of MMPs by macrophages and smooth muscle cells likely contributes to weakening of the vascular wall via their capacity to cleave extracellular matrix (ECM). Thus far, the role of MMPs in atherosclerosis has been mainly investigated using transgenic or knock-out mice but the results can be confusing[1]. For example, MMP inhibition by genetic deletion of one of the MMP genes or by a pharmacological intervention using an MMP inhibitor decreased aneurysm and neointima formation[1]. Yet, overexpression of MMP-1 resulted in a decreased plaque size, inhibition of MMP-3 led to an increase in plaque size and plaque progression, while broad range MMP inhibitors had no effect on plaque size. Thus, interventions aimed at altering MMP expression/activity revealed the complexity of the regulation of ECM turnover and that actions of certain members of the MMP family may be redundant or compensatory in nature.

Whereas the literature on MMPs and cardiovascular phenotypes in animal models is extensive[1], their vascular substrates have not been comprehensively characterized. MMPs tend to be grouped into interstitial collagenases (MMPs-1, -8, -13, -14) that cleave fibrillar collagens, gelatinases (MMPs-2 and -9) that efficiently cleave denatured collagen (i.e. gelatin) and stromelysins (MMPs-3, -7, -10, -11) that have a broad specificity but do not cleave intact fibrillar collagen[2]. In this study, we attempt to gain a more comprehensive picture by employing a proteomics approach. We identify candidate substrates for three MMPs, one from each of the three major classes of MMPs: MMP-3, MMP-9 and MMP-14. All three MMPs are implicated in cardiovascular pathologies: MMP-14 (a membrane-bound MMP) is induced in macrophages by

oxidized lipoproteins and degrades a broad range of substrates in the pericellular regions including other MMPs[3]. Similarly, macrophages as well as vascular smooth muscle cells secrete MMP-9 after inflammatory activation[4]. Levels of MMP-9 are increased in atherosclerotic plaques with histological features of vulnerability to rupture[5]. MMP-3 as well as other stromelysins are considered to display the broadest substrate specificity. Functional genetic polymorphisms present in the MMP-3 promoters have been associated with atherosclerosis progression and the risk of abdominal aortic aneurysms as reviewed elsewhere[1].

Methods

Source of tissue. Human radial arteries were obtained from three male patients >50 yrs of age undergoing coronary bypass surgery. Four human aortas were obtained from patients without connective tissue disorder (one female and three males ages 20 to 55) upon aortotomy performed during routine aortic valve replacement from positions of the ascending aorta. The study was approved by St. George's Hospital and the National Research Ethics Service Committee London – Wandsworth. Patients gave written informed consent.

Digestion with MMPs. Before extraction the tissue were partially thawed and weighed. Approximately 120mg tissue was first washed with ice-cold PBS (Lonza, Belgium) containing protease and phosphatase inhibitor (Sigma-Aldrich). The tissue was diced into five pieces of ~ 20mg and washed three times with PBS before a final wash with 1mL MMP reaction buffer (10mM $CaCl_2$, 120mM NaCl, 50mM Tris, pH = 9.0, containing 10μL protease and phosphatase inhibitors). For digestion, each sample (n=5) was incubated in MMP reaction buffer at 37°C. The volume of the buffer was adjusted to 10:1 of the tissue weight and included 3μL of protease inhibitor per sample. One sample was used as control to monitor background MMP activity and

incubated only in buffer with protease inhibitor (for inhibition of endogenous proteases, other than MMPs). A second control was incubated in buffer with protease inhibitor plus 25mM EDTA (Sigma-Aldrich) to ensure inhibition of MMPs. The three remaining samples were incubated with 10µg/ml MMP-3, MMP-9 (Calbiochem) or MMP-14 (R&D Systems) at 100ng MMP/mg arterial tissue. MMP-14 was activated with furin (R&D Systems) according to the manufacturer's protocol. Furin was then inactivated before further experiments. After 28h incubation with radial arterial tissue, the supernatant was transferred in new tubes and released proteins were deglycosylated in deglycosylation buffer (150mM NaCl, 50mM sodium acetate, 25mM EDTA, pH=6.8) containing chondroitinase ABC from *Proteus vulgaris* and keratanase from *Pseudomonas sp.* (both Sigma-Aldrich). After an overnight incubation at 37°C, samples were concentrated by vacuum centrifugation for 30min and the protein concentration was estimated by UV absorbance at 280nm using a NanoDrop ND-1000 (Thermo Scientific).

SDS-PAGE. 4x sample buffer (100mM Tris, pH=6.8, containing 40% glycerol, 0.2% SDS, 2% beta-mercaptoethanol, 0.02% bromophenol blue) was added to 45µg of protein. After boiling (5min at 96°C), samples were separated together with a protein standard (All Blue, Precision, Bio-Rad Laboratories) on Bis-Tris 4-12% polyacrylamide gradient gels (NuPage, Life-Technologies).

Liquid chromatography tandem mass spectrometry (LC-MS/MS). Gels were stained with Coomasie G-250. Sixteen bands were excised per lane, destained, reduced, alkylated, and digested with Sequencing Grade Modified Trypsin (Promega) using an Investigator ProGest (Genomic Solutions) robotic digestion system. Peptides were analysed by LC-MS/MS as described[6, 7]. Tryptic peptides were separated by reverse phase chromatography (Acclaim PepMap100 C18, 75µm x 15cm) on a nanoflow LC system (Ultimate3000, Dionex) equipped

with a trap column (Acclaim PepMap100 C18, 300µm x 5 mm). The chromatographic separation was performed with a mobile phase of HPLC grade water containing 2% acetonitrile and 0.1% formic aid (eluent A) and a solvent phase of acetonitrile containing 10% HPLC water (Fisher Scientific) and 0.1% formic acid (eluent B) with a 90min gradient (10-25%B in 55min, 55-60%B in 5min, 90%B for 8min, 90-2%B in 22min) at a flow rate of 300nL/min. The column was coupled to a LTQ OrbitrapXL mass spectrometer (Thermo Fisher Scientific) with a nanospray source (Picoview). The mass spectrometry acquisition involved one full MS scan, over a mass range encompassing 450-1600Da, followed by data-dependent CID MS/MS scans of the 6 most intense ions detected in the full scan, with dynamic exclusion enabled and rejection of singly charged ions.

Data analysis. Mascot Daemon (Matrix Science, London, UK; version 2.3.0) was used to extract each raw data file into a set of DTA files, which were merged into MGF files. These files were searched against a subset (human, 20266 entries) of the UniProtKB/Swiss-Prot database (SwissProt_57.15) using Mascot (Matrix Science, London, UK; version 2.3.01). A mass tolerance of 10ppm for precursor ion scans, and a mass tolerance of 0.8Da for the product ion scans was used. Semi-trypsin with up to two missed cleavage sites was chosen as enzymatic cleavage to identify non-tryptic MMP cleavage sites. Iodoacetamide derivative of cysteine was specified as a fixed modification, hydroxylation of proline and lysine and oxidation of methionine were specified as variable modifications. Scaffold (version Scaffold_3_00_02, Proteome Software Inc., Portland, OR) was used to calculate the spectral counts and to validate MS/MS based peptide and protein identifications: peptide identifications were accepted if they could be established at greater than 95.0% probability; protein identifications were accepted if they could be established at greater than 99.0% probability with at least two independent

identified peptides and a mass accuracy of ≤10ppm of the precursor ion.

Western Blotting. Proteins were transferred to nitrocellulose (GE Healthcare). Membranes were blocked in 5% fat-free milk powder in PBS and probed for 16h at 4°C with antibodies purchased from Santa Cruz Biotechnology (Santa Cruz, CA) or Abcam (Cambridge, UK): tenascin-C (ab6393), periostin (sc-67233), galectin-1 (ab38328), fibronectin (sc-56391) and tenascin-X (sc-25717). Primary antibodies were used at a 1:500 dilution in 5% BSA (Sigma-Aldrich). Secondary, peroxidase-conjugated antibodies (Dako, Glostrup, Denmark) were used at a 1:1500 dilution. Using enhanced chemiluminescence (ECL; GE Healthcare), films were developed on a Xograph processor (Tetbury, UK).

Recombinant proteins. 10μg of periostin (both R&D Systems), fibronectin (Sigma) and tenascin-C (Millipore) were incubated with MMP-3, MMP-9 and MMP-14 at a molar protein/MMP ratio of 10:1 for 16h at 37°C. Controls were incubated without MMPs. Reactions were terminated by addition of EDTA (final concentration 25mM). Periostin, fibronectin, and tenascin-C were analyzed by SDS-PAGE using MOPS running buffer and stained with Colloidal Blue (Life-Technologies). In addition, all recombinant proteins were reduced, alkylated, digested with trypsin at 37°C over night and analyzed directly without prior gel separation by LC-MS/MS.

Statistical analysis. The differential expression analysis was performed using the *Qspec* method as described by Choi *et al* [8]. *Qspec* utilises a model based on a hierarchical Bayes estimation of generalized linear mixed effects model (GLMM) to calculate the differential expression. Here, 100,000 iterations were used with a 10,000-iteration burn in for the MCMC parameter estimation. The statistical significance is indicated by Bayes factors and the associated False Discovery Rates were calculated with a mixture model-based method of controlling the local

FDR. The *Qspec* method also accounts for the length of the protein when determining the differential expression. Values reported are spectral counts for each protein calculated as average±S.E. of 3 biological replicates samples. All assigned spectra for each protein were used for spectral counting. Before statistical analysis protein spectral counts were normalized using the Scaffold software (version3_00_02, Proteome Software Inc., Portland, OR) by calculating and averaging the number of identified spectra in each sample, then multiplying the number of spectra assigned to each protein by the ratio of the average spectral count to the number of total spectra in that sample. Protein ambiguity issues were handled using tools available in the Scaffold software. Only proteins identified with at least two unique peptides were included in the analysis. No outliers were removed.

Results

Proteomic analysis. Human radial arteries macroscopically free of vascular disease were diced into small pieces and subjected to overnight incubation with MMP-3, MMP-9 or MMP-14 (100ng MMP/mg tissue at 37°C plus proteinase inhibitors to inhibit proteinases other than MMPs). Radial arteries incubated in MMP-buffer with or without EDTA served as control. The proteins released into the conditioned medium were concentrated and separated by SDS-PAGE. The entire lane was excised, subjected to in-gel tryptic digestion and analysed by LC-MS/MS using a high-resolution mass spectrometer (LTQ Orbitrap XL, ThermoFisher). All further analysis focused on 99 ECM or ECM-related proteins (13 proteoglycans, 36 ECM glycoproteins, 14 collagens, 5 non-glycosylated ECM proteins, 19 other ECM-associated proteins, 12 proteases & protease inhibitors) identified with 95% peptide probability, 99% protein probability, 10ppm mass accuracy and a minimum of two peptides per protein (see online-only Data **Supplemental Table 1)**. Three collagens (COSA1_HUMAN, COGA1_HUMAN, CO1A1_HUMAN) were only

found when hydroxy-lysine and hydroxy–proline were chosen as variable modifications. All detected ECM and ECM-related proteins are listed in **Table 1.**

Increased release upon digestion by MMPs. Among the identified extracellular proteins, 25 proteins were differentially released upon digestion by MMPs (**Table 1**), including known MMP substrates like fibronectin (FINC)[9], collagens[10], and perlecan (PGBM)[9, 11] (see online-only Data **Supplemental Table 2**) as well as unknown ones, like EMILIN-1 (EMIL1) and tenascin-X (TENX) (**Figure 1**). For some MMP substrates, our study revealed release by additional MMPs, e.g. CO6A3 by MMP-3 and 9 (known substrate for MMP-2[12]). For others, e.g. tenascin-C (TENA, known substrate for MMP-3 and 14) statistical significance was obtained for MMP-3, but not for MMP-14. Protein fragments of very small proteins such as galectin-1 (LEG1) were migrating ahead of the gel front thereby resulting in a reduced spectral count upon digestion **(Table 1)**. For independent validation of the proteomic findings, the samples were probed for fibronectin, galectin-1, tenascin-C, periostin, and tenascin-X by immunoblotting **(Figure 2)**. Indeed, immunoblots confirmed the degradation of galectin-1 by MMP-3 with the cleaved products close to the migration front on the SDS-PAGE. Consistent with the published literature[13], degradation was also observed with MMP-9, but to a lesser extent. In contrast, we observed no cleavage with MMP-14[14].

Evidence for protein fragmentation. Proteolytic cleavage may occur without differential release into the conditioned medium, e.g. for aggrecan (known substrate for MMP-3, 9, 14) or nidogen-1 (known substrate for MMP-3, 9, 14). Separation by SDS-PAGE prior to tryptic digestion preserves the native molecular weight of the protein. Detailed examination of the gel-LC-MS/MS data revealed the presence of proteolytic products after incubation with MMPs: For aggrecan, nidogen-1, fibronectin, periostin, perlecan, tenascin-C, and tenascin-X, a high number

of MS/MS spectra were identified in gel segments below the expected molecular weight of the native protein (**Figure 3**). To further investigate MMP-dependent proteolysis, additional specimens of radial arteries were incubated with two different concentrations of MMPs: 20 ng MMP/mg tissue (L – low) and 100 ng MMP/mg tissue (H - high) (**Figure 4,** upper panel). EDTA was added as negative control for inhibition of MMP activity (**Figure 4,** lower panel). In agreement with the proteomics findings and the published literature[9, 15], fibronectin was degraded by MMP-3 and -14 and to a lesser extent by MMP-9. Tenascin-X, a new substrate for MMPs, was cleaved by MMP-3, -9 and -14. In contrast, tenascin-C was predominantly degraded by MMP-3 and to some extent by -14, but not by MMP-9. This has been previously reported in the literature based on *in vitro* studies using purified proteins[9, 16, 17]. Our study provides the first evidence for cleavage of tenascin-C by MMP-3 and -14 in human arterial tissue. Similarly, MMP-3 and MMP-14 cleaved periostin, another potential new substrate for both MMPs. As direct evidence, recombinant or purified fibronectin, tenascin-C and periostin were incubated with MMP-3, -9 and -14 and the cleavage products were analysed by SDS-PAGE. Fibronectin, a known substrate of MMPs, was cleaved by all three MMPs (**Figure 5A**). Tenascin-C (**Figure 5B**) and periostin (**Figure 5C**) were degraded by MMP-3.

Identification of cleavage sites. Next, all spectra were searched for non-tryptic cleavages sites. Endogenous proteases, other than MMPs, were inhibited by addition of a proteinase inhibitor cocktail. 74 semi-tryptic peptides (66 peptides were cleaved by MMP-3, 12 by MMP-9 and 12 by MMP-14) were identified in at least two out of three radial arteries digested with MMPs, but undetectable in controls (**Figure 6,** see online-only Data **Supplement Table 3**). Two MMP cleavage sites were already known from the literature[18], namely cleavage of biglycan (ISE^{114}↓LRK) (see online-only Data **Supplement Figure 2**) by MMP-3, -9, and -13 and

cleavage of fibronectin (PIQ↓^{630}WNA) (see online-only Data **Supplement Figure 3**) by MMP-3, -9 and -12 supporting the validity of our proteomics approach. Five cleavage sites reported for other MMPs were also cleaved by MMP-3, -9, and/or 14. For example, fibronectin PSQ↓^{1548}MQV (a known cleavage product of MMP-2 [19]) was identified after incubation with MMP-3 (see online-only Data **Supplement Figure 4**). N-terminal cleavage of galectin-1 (ACG↓^{5}LVA, a known substrate of MMP-2[13] and MMP-9[19]) was observed upon digestion with MMP-3 and -14 (see online-only Data **Supplement Figure 5**). Cleavage of prolargin (PRN^{172}↓LEQ, a known substrate by MMP-8 and -12[18]) was identified with MMP-14 (see online-only Data **Supplement Figure 6**). The important cleavage site in collagen XVIII (VVQ^{1511}↓LHD, COIA1_HUMAN), cleaved by MMP-7 to generate endostatin[20], was detected upon incubation with MMP-3 and 14 (see online-only Data **Supplement Figure 7**). Two other collagen cleavage sites, PGQ^{639}↓^{640}LQG (CO3A1_HUMAN, a known substrate for MMP-9 and -13[3]) (see online-only Data **Supplement Figure 8**) as well as PPG^{645}↓^{646}FLG (CO4A2_HUMAN, see online-only Data **Supplement Figure 9**), were confirmed by two complimentary semi-tryptic peptides. The highest number of non-tryptic cleavage sites was returned for fibronectin. For validation, an in-solution digest of the recombinant / purified proteins were analysed directly by LC-MS/MS: 8 out of 21 cleavage sites for fibronectin were confirmed (see online-only Data **Supplement Figure 10**). In addition, we were able to detect 27 non-tryptic cleavage sites in periostin (see online-only Data **Supplement Figure 11**) and 12 non-tryptic cleavage sites for tenascin-C (see online-only Data **Supplement Figure 12**).

Evidence for protein degradation in human aortic tissue. We have previously established a three-step extraction procedure for the proteomic identification of ECM proteins in human thoracic aortas (**Figure 7A**)[21]. In tissues, proteolytic degradation products are present in the NaCl

fraction. As described, the different levels of endogenous MMP-9 activity (**Figure 7B**) correlated to fibronectin degradation, a well-known substrate of MMP-9. When we re-analysed this proteomics dataset for evidence of degradation of novel candidate substrates identified by incubation with exogenous MMP-9 (**Figure 7C**), degradation was evident for collagen VI (CO6A3), collagen XV (COFA1), serum amyloid P-component (SAMP) and latent TGF-binding protein 2 (LTBP2) (**Figure 7D**). Fragmentation of collagen VI was independently confirmed by immunoblotting (**Figure 7E**).

Discussion

Proteolysis is a key mechanism to control ECM function during development and normal tissue turnover. To advance our understanding of ECM remodeling in disease, we have established proteomics methods to analyse the ECM composition in human aortas[21], abdominal aortic aneurysms[22] and after cardiac ischemia/reperfusion injury[7]. In these studies, the most abundant MMPs were detected, but a more detailed knowledge of their substrates is essential to link MMP activity to ECM changes in cardiovascular disease. Since MMPs do not hydrolyze peptide bonds in sequence-specific manner, proteomics offers an opportunity for a comprehensive assessment of MMP substrates[23, 24].

Degradomics. The 'degradome' is the complete natural substrate repertoire of a protease in a cell, tissue or organism[25]. Different MS-based approaches can be used for the identification of new MMP substrates and their cleavage sites, such as iCAT or iTRAQ[26], label-free MS[27], and 2D gel electrophoresis[28]. For the degradome of a certain subset of proteins, peptide libraries[29,30] generate maps of potential cleavage sites for the protease of interest. Other proteomic approaches, like TAILS, COFRADIC and PROTOMAP were developed for an enrichment and identification of new N-terminal peptides to identify specific protease cleavage sites[31-33]. A

limitation of such *in vitro* approaches is the overestimation of the actual cleavage sites, since certain proteins may be inaccessible to the protease in a tissue environment. *In vivo* studies on MMPs relied heavily on comparisons of cardiovascular phenotypes in transgenic and wildtype animals[1]. Potential caveats are that genetic manipulations frequently induce secondary changes. For example, we have previously shown that aortas of apoE-deficient mice show low levels of ADAMTS-5 compared to wildtype controls[34]. This loss of ADAMTS-5 may be important for proteoglycan accumulation and lipoprotein retention[35]. Alterations in other proteases, however, complicate the interpretation of experiments with loss or gain of function for specific MMPs in apoE-deficient mice, and the clinical relevance of such findings ought to be further substantiated in human tissue.

Combined *ex vivo / in vivo* approach. Strengths of our study are the extensive proteomics analyses and the use of human arterial tissues: To identify MMP substrates, we compared the protein release from vascular tissues after incubation with three different MMPs. Evidence for protein fragmentation was collated from the gel-LC-MS/MS experiment. Then, mass spectra were searched for non-tryptic peptides to identify MMP cleavage sites (see online-only Data **Supplemental Table 3**). For most candidate substrates, non-tryptic peptides were detected providing evidence that these proteins are indeed undergoing proteolytic cleavage upon incubation with MMPs. As proof-of-principle, newly identified targets were confirmed by immunoblotting and by digesting recombinant / purified proteins. Finally, our findings were related to human tissues with different levels of endogenous MMP activities, as reported for articular cartilage[18] and abdominal aortic aneurysms[22]. Novel candidate substrates identified by incubating arterial tissue with exogenous MMP-9 also displayed evidence for degradation in aortic tissues with high endogenous MMP-9 activity.

Novel MMP substrates. MMP-3 but also MMP-9 cleaved numerous ECM proteins, predominantly in the basement membrane and the interstitial matrix. Among the basement membrane proteins identified were collagen IV, XV, XVIII, nidogen, and perlecan (PGBM). Collagen XV (COFA1) was also degraded in aortic tissues with high MMP-9 activity. Collagen IV and perlecan are known MMP substrates (see online-only Data **Supplemental Table 2**), but our study identified new cleavage sites. In all experiments, collagen VI was consistently emerged as a novel substrate for MMP-9. Type VI collagen is one of the main components of interstitial matrix and particularly enriched in the pericellular matrix as well as the subendothelial matrix that binds von Willebrand factor and platelets. Collagen forming reticular fibers (collagen III) and proteins associated with elastic fibres (EMIL1, and LTBP2) were also detected. Elastic fibres are composed of the protein elastin and a network of microfibrils, consisting of several glycoproteins, including fibrillin-1, fibrillin-2, and microfibril-associated glycoproteins-1 and -2 [36]. Notably, MMP-3 and -9 degrade elastic fiber proteins and damage to these structures can negatively affect the quality of the elastin network and impair vascular function[37].

Periostin and tenascins, in particular tenascin-X, were shown to be new MMP substrates. Tenascins are matricellular proteins that bind to ECM proteins and cell surface receptors without contributing to the structure of the ECM itself. Tenascin-X is an important regulator of collagen deposition by dermal fibroblasts[38]. In contrast, tenascin-C binds to fibronectin and inhibits cell spreading[39]. It is related to macrophage accumulation in vascular lesions[40], increases the activity of MMPs and is present in the vulnerable region of atherosclerotic plaques. The incorporation of tenascin-C into the ECM is promoted by periostin[41], a 90kDa secreted protein, which plays a role in vascular cell differentiation and migration[42]. We have previously identified periostin as a substrate of MMP-12[22]. This study demonstrates that periostin is also cleaved by MMP-3.

Among the group of large aggregating proteoglycans, aggrecan was only recently detected in human arteries[43]. Our study now demonstrates its fragmentation upon incubation with MMP-3 and -9.

Novel cleavage sites. For many known substrates, we identified potential new cleavage sites. Importantly, ECM fragments can have biological activity or contain biologically active sites that are not present or exposed in the original molecule. Such 'cryptic' sites are known for some collagens (like endostatin, which inhibits endothelial cell proliferation and angiogenesis)[44] as well as fibronectin[45], to name just a few. Fibronectin, for example, is one of the most prominent ECM proteins accumulating in atherosclerosis. The potential biological activity of the newly identified ECM fragments will have to be explored in future studies.

Limitations. Although a single MMP can have potent effects on the ECM, more complex processes involving the interplay of different MMPs and their inhibitors are taking place *in vivo*. This diminishes the power of tissue proteomics in identifying direct substrates of MMPs: 1) It is known that MMPs can activate other MMPs, for example MMP-3 activates MMP-9[46]. Thus, incubation with exogenous MMPs is likely to activate endogenous MMPs. This is impossible to overcome in human tissues but all our buffers were supplemented with a proteinase inhibitor mixture to inhibit non-MMP proteinase activity; 2) Proteins might be released that were just bound to substrates of MMPs. So, the mere solubilization of proteins upon digestion is insufficient to designate proteins as direct substrates of MMPs. Nonetheless, evidence of proteolytic degradation (**Figures 3** and **5**) and certain cleavage sites (**Figures 6**) were independently observed in tissues as well as in recombinant / purified proteins. 3) The analysis was filtered for extracellular proteins because arteries were snap-frozen after collection. Cells may burst during the freezing process. Thus, interpreting the release of cellular proteins upon

digestion with MMPs might not be reliable.

Conclusion

This proteomics study will provide a valuable resource for scientists investigating pathophysiological consequences of MMP activity. For the first time, it characterizes the overall effect of these important matrix-degrading enzymes in the human vasculature. Ultimately, such comparisons of different MMP activities may help to elucidate the mechanisms of plaque destabilization and aneurysm formation and identify new culprit molecules that could be targeted for therapy[1, 47].

Acknowledgments: We thank Dr. Xiaoke Yin and Dr. Ursula Mayr for technical assistance.

Funding Sources: This work was funded by the Department of Health via a National Institute for Health Research (NIHR) Biomedical Research Centre award to Guy's and St. Thomas' NHS Foundation Trust in partnership with King's College London and King's College Hospital NHS Foundation Trust. M.M. is a Senior Fellow of the British Heart Foundation. M.M. is a Senior Fellow of the British Heart Foundation.

Conflict of Interest Disclosures: None.

References:

1. Newby AC. Matrix metalloproteinase inhibition therapy for vascular diseases. *Vascul Pharmacol*. 2012;56:232-244.

2. Nagase H, Woessner JF, Jr. Matrix metalloproteinases. *J Biol Chem*. 1999;274:21491-21494.

3. Ray BK, Shakya A, Turk JR, Apte SS, Ray A. Induction of the mmp-14 gene in macrophages of the atherosclerotic plaque: Role of saf-1 in the induction process. *Circ Res*. 2004;95:1082-1090.

4. Newby AC. Matrix metalloproteinases regulate migration, proliferation, and death of vascular smooth muscle cells by degrading matrix and non-matrix substrates. *Cardiovasc Res*. 2006;69:614-624.

5. Sluijter JP, Pulskens WP, Schoneveld AH, Velema E, Strijder CF, Moll F, et al. Matrix metalloproteinase 2 is associated with stable and matrix metalloproteinases 8 and 9 with vulnerable carotid atherosclerotic lesions: A study in human endarterectomy specimen pointing to a role for different extracellular matrix metalloproteinase inducer glycosylation forms. *Stroke*. 2006;37:235-239.

6. Yin X, Cuello F, Mayr U, Hao Z, Hornshaw M, Ehler E, et al. Proteomics analysis of the cardiac myofilament subproteome reveals dynamic alterations in phosphatase subunit distribution. *Mol Cell Proteomics*. 2010;9:497-509.

7. Barallobre-Barreiro J, Didangelos A, Schoendube FA, Drozdov I, Yin X, Fernandez-Caggiano M, et al. Proteomics analysis of cardiac extracellular matrix remodeling in a porcine model of ischemia/reperfusion injury. *Circulation*. 2012;125:789-802.

8. Choi H, Fermin D, Nesvizhskii AI. Significance analysis of spectral count data in label-free shotgun proteomics. *Mol Cell Proteomics*. 2008;7:2373-2385.

9. d'Ortho MP, Will H, Atkinson S, Butler G, Messent A, Gavrilovic J, et al. Membrane-type matrix metalloproteinases 1 and 2 exhibit broad-spectrum proteolytic capacities comparable to many matrix metalloproteinases. *Eur J Biochem*. 1997;250:751-757.

10. Murphy G, Reynolds JJ, Bretz U, Baggiolini M. Partial purification of collagenase and gelatinase from human polymorphonuclear leucocytes. Analysis of their actions on soluble and insoluble collagens. *Biochem J*. 1982;203:209-221.

11. Whitelock JM, Murdoch AD, Iozzo RV, Underwood PA. The degradation of human endothelial cell-derived perlecan and release of bound basic fibroblast growth factor by stromelysin, collagenase, plasmin, and heparanases. *J Biol Chem*. 1996;271:10079-10086

12. Myint E, Brown DJ, Ljubimov AV, Kyaw M, Kenney MC. Cleavage of human corneal type vi collagen alpha 3 chain by matrix metalloproteinase-2. *Cornea*. 1996;15:490-496.

13. Prudova A, auf dem Keller U, Butler GS, Overall CM. Multiplex n-terminome analysis of mmp-2 and mmp-9 substrate degradomes by itraq-tails quantitative proteomics. *Mol Cell Proteomics*. 2010;9:894-911.

14. Butler GS, Dean RA, Tam EM, Overall CM. Pharmacoproteomics of a metalloproteinase hydroxamate inhibitor in breast cancer cells: Dynamics of membrane type 1 matrix metalloproteinase-mediated membrane protein shedding. *Mol Cell Biol*. 2008;28:4896-4914.

15. Fukai F, Ohtaki M, Fujii N, Yajima H, Ishii T, Nishizawa Y et al. Release of biological activities from quiescent fibronectin by a conformational change and limited proteolysis by matrix metalloproteinases. *Biochemistry*. 1995;34:11453-11459.

16. Imai K, Kusakabe M, Sakakura T, Nakanishi I, Okada Y. Susceptibility of tenascin to degradation by matrix metalloproteinases and serine proteinases. *FEBS Lett*. 1994;352:216-218.

17. Siri A, Knauper V, Veirana N, Caocci F, Murphy G, Zardi L. Different susceptibility of small and large human tenascin-c isoforms to degradation by matrix metalloproteinases. *J Biol Chem*. 1995;270:8650-8654.

18. Zhen EY, Brittain IJ, Laska DA, Mitchell PG, Sumer EU, Karsdal MA et al. Characterization of metalloprotease cleavage products of human articular cartilage. *Arthritis Rheum*. 2008;58:2420-2431.

19. auf dem Keller U, Prudova A, Gioia M, Butler GS, Overall CM. A statistics-based platform for quantitative n-terminome analysis and identification of protease cleavage products. *Mol Cell Proteomics*. 2010;9:912-927.

20. Ferreras M, Felbor U, Lenhard T, Olsen BR, Delaisse J. Generation and degradation of human endostatin proteins by various proteinases. *FEBS Lett*. 2000;486:247-251.

21. Didangelos A, Yin X, Mandal K, Baumert M, Jahangiri M, Mayr M. Proteomics characterization of extracellular space components in the human aorta. *Mol Cell Proteomics*. 2010;9:2048-2062.

22. Didangelos A, Yin X, Mandal K, Saje A, Smith A, Xu Q et al. Extracellular matrix composition and remodeling in human abdominal aortic aneurysms: A proteomics approach. *Mol Cell Proteomics*. 2011;10:M111.008128.

23. Klingler D, Hardt M. Targeting proteases in cardiovascular diseases by mass spectrometry-based proteomics. *Circ Cardiovasc Genet*. 2012;5:265.

24. Didangelos A, Stegemann C, Mayr M. The -omics era: Proteomics and lipidomics in vascular research. *Atherosclerosis*. 2012;221:12-17.

25. Lopez-Otin C, Overall CM. Protease degradomics: A new challenge for proteomics. *Nat Rev Mol Cell Biol*. 2002;3:509-519.

26. Tam EM, Morrison CJ, Wu YI, Stack MS, Overall CM. Membrane protease proteomics: Isotope-coded affinity tag ms identification of undescribed mt1-matrix metalloproteinase substrates. *Proc Natl Acad Sci U S A*. 2004;101:6917-6922.

27. Vaisar T, Kassim SY, Gomez IG, Green PS, Hargarten S, Gough PJ et al. Mmp-9 sheds the beta2 integrin subunit (cd18) from macrophages. *Mol Cell Proteomics*. 2009;8:1044-1060.

28. Greenlee KJ, Corry DB, Engler DA, Matsunami RK, Tessier P, Cook RG, et al. Proteomic identification of in vivo substrates for matrix metalloproteinases 2 and 9 reveals a mechanism for resolution of inflammation. *J Immunol*. 2006;177:7312-7321.

29. Schilling O, Overall CM. Proteome-derived, database-searchable peptide libraries for identifying protease cleavage sites. *Nat Biotechnol*. 2008;26:685-694.

30. Schilling O, Huesgen PF, Barre O, Auf dem Keller U, Overall CM. Characterization of the prime and non-prime active site specificities of proteases by proteome-derived peptide libraries and tandem mass spectrometry. *Nat Protoc*. 2011;6:111-120.

31. Dix MM, Simon GM, Cravatt BF. Global mapping of the topography and magnitude of proteolytic events in apoptosis. *Cell*. 2008;134:679-691.

32. Gevaert K, Goethals M, Martens L, Van Damme J, Staes A, Thomas GR, et al. Exploring proteomes and analyzing protein processing by mass spectrometric identification of sorted n-terminal peptides. *Nat Biotechnol*. 2003;21:566-569.

33. Kleifeld O, Doucet A, auf dem Keller U, Prudova A, Schilling O, Kainthan RK, et al. Isotopic labeling of terminal amines in complex samples identifies protein n-termini and protease cleavage products. *Nat Biotechnol*. 2010;28:281-288.

34. Didangelos A, Mayr U, Monaco C, Mayr M. Novel role of adamts-5 protein in proteoglycan turnover and lipoprotein retention in atherosclerosis. *J Biol Chem*. 2012;287:19341-19345.

35. Stegemann C, Drozdov I, Shalhoub J, Humphries J, Ladroue C, Didangelos A et al. Comparative lipidomics profiling of human atherosclerotic plaques. *Circ Cardiovasc Genet*. 2011;4:232-242.

36. Kielty CM, Sherratt MJ, Shuttleworth CA. Elastic fibres. *J Cell Sci*. 2002;115:2817-2828.

37. Van Herck JL, De Meyer GR, Martinet W, Van Hove CE, Foubert K, Theunis MH et al. Impaired fibrillin-1 function promotes features of plaque instability in apolipoprotein e-deficient mice. *Circulation*. 2009;120:2478-2487.

38. Mao JR, Taylor G, Dean WB, Wagner DR, Afzal V, Lotz JC et al. Tenascin-x deficiency mimics ehlers-danlos syndrome in mice through alteration of collagen deposition. *Nat Genet*. 2002;30:421-425.

39. Huang W, Chiquet-Ehrismann R, Moyano JV, Garcia-Pardo A, Orend G. Interference of tenascin-c with syndecan-4 binding to fibronectin blocks cell adhesion and stimulates tumor cell proliferation. *Cancer Res*. 2001;61:8586-8594.

40. Wallner K, Li C, Shah PK, Fishbein MC, Forrester JS, Kaul S et al. Tenascin-c is expressed in macrophage-rich human coronary atherosclerotic plaque. *Circulation*. 1999;99:1284-1289.

41. Maruhashi T, Kii I, Saito M, Kudo A. Interaction between periostin and bmp-1 promotes proteolytic activation of lysyl oxidase. *J Biol Chem*. 2010;285:13294-13303.

42. Lindner V, Wang Q, Conley BA, Friesel RE, Vary CP. Vascular injury induces expression of periostin: Implications for vascular cell differentiation and migration. *Arterioscler Thromb Vasc Biol*. 2005;25:77-83.

43. Talusan P, Bedri S, Yang S, Kattapuram T, Silva N, Roughley PJ et al. Analysis of intimal proteoglycans in atherosclerosis-prone and atherosclerosis-resistant human arteries by mass spectrometry. *Mol Cell Proteomics*. 2005;4:1350-1357.

44. Marneros AG, Olsen BR. The role of collagen-derived proteolytic fragments in angiogenesis. *Matrix Biol*. 2001;20:337-345.

45. Schenk S, Quaranta V. Tales from the crypt[ic] sites of the extracellular matrix. *Trends Cell Biol*. 2003;13:366-375.

46. Ogata Y, Enghild JJ, Nagase H. Matrix metalloproteinase 3 (stromelysin) activates the precursor for the human matrix metalloproteinase 9. *J Biol Chem*. 1992;267:3581-3584.

47. Arrell DK, Terzic A. Systems proteomics for translational network medicine. *Circ Cardiovasc Genet.* 2012;5:478.

DOI: 10.1161/CIRCGENETICS.112.964452

Table 1. Extracellular proteins released from human arteries upon incubation with MMP-3, -9 and -14.

Protein	Swiss prot	Control (-EDTA)	Control (+EDTA)	MMP-3	MMP-9	MMP-14
Proteoglycans (13)						
Aggrecan	PGCA_HUMAN	43±12	32±6	57±27	70±45	40±4
Agrin	AGRIN_HUMAN	1±1	1±1	4±1	3±3	3±4
Biglycan[#]	PGS1_HUMAN	32±14	13±6	**21±13***	28±22	33±17
Chondroitin sulfate proteoglycan 4	CSPG4_HUMAN	10±10	4±2	24±14	14±5	14±4
Decorin	PGS2_HUMAN	20±15	21±6	13±2	22±15	24±29
Fibromodulin	FMOD_HUMAN	3±2	3±1	4±3	8±7	10±11
Glypican-1	GPC1_HUMAN	4±3	3±3	3±1	4±2	2±1
Glypican-4	GPC4_HUMAN	1±1	1±1	1±0	1±0	2±1
Lumican	LUM_HUMAN	52±29	32±17	39±1	54±34	45±36
Mimecan	MIME_HUMAN	39±7	10±3	**12±7*****	29±12	**26±12****
Perlecan[#]	PGBM_HUMAN	94±74	103±48	**794±29*****	**370± 208*****	**402±7*****
Prolargin	PRELP_HUMAN	35±21	28±4	27±13	39±9	46±17
Versican core protein	CSPG2_HUMAN	124±47	100±27	142±89	194±141	139±92
ECM Glycoproteins (36)						
Adipocyte enhancer-binding protein 1	AEBP1_HUMAN	11±5	17±4	13±11	13±11	18±16
Cartilage intermediate layer protein 1	CILP1_HUMAN	3±1	1±0	3±2	1±1	1±1
Cartilage oligomeric matrix protein	COMP_HUMAN	8±8	8±6	8±4	**26±23***	10±7
Ceruloplasmin	CERU_HUMAN	20±21	18±14	14±7	16±8	20±11
Clusterin	CLUS_HUMAN	20±5	14±3	19±10	18±8	16±5
EGF-containing fibulin-like ECM protein 1	FBLN3_HUMAN	53±17	44±12	63±48	70±71	53±46
EMILIN-1	EMIL1_HUMAN	4±4	1±1	**39±7*****	**15±5*****	**15±6*****
Fibrillin-1	FBN1_HUMAN	1±1	24±21	39±15	2±1	1±0
Fibronectin[#]	FINC_HUMAN	73±61	30±16	**468±152*****	**133±65*****	**184±26***
Fibulin-1	FBLN1_HUMAN	16±20	20±14	37±35	35±31	20±25
Fibulin-2	FBLN2_HUMAN	1±1	25±20	25±6	8±4	1±1
Fibulin-5	FBLN5_HUMAN	2±2	6±4	7±5	4±5	3±4
Lactadherin	MFGM_HUMAN	10±10	11±9	8±8	9±8	7±4
Laminin subunit α-4	LAMA4_HUMAN	1±1	1±0	1±1	1±1	1±1
Laminin subunit α-5[#]	LAMA5_HUMAN	5±3	3±3	**52±43*****	22±18	**20±13*****
Laminin subunit α-1	LAMB1_HUMAN	0±1	1±1	2±2	1±1	1±1
Laminin subunit β-2	LAMB2_HUMAN	19±17	5±5	49±43	31±28	20±17
Laminin subunit γ-1	LAMC1_HUMAN	29±25	20±17	50±45	31±27	30±29
Latent-TGF β-binding protein 1	LTBP1_HUMAN	1±1	2±1	19±5	1±0	5±7

DOI: 10.1161/CIRCGENETICS.112.964452

Latent-TGF β-binding protein 2	LTBP2_HUMAN	8±6	10±5	**35±22*** **	**22±2***	**35±19*** **
Latent-TGF β-binding protein 4	LTBP4_HUMAN	9±7	3±2	19±7	8±8	6±4
Matrilin-2	MATN2_HUMAN	1±1	1±1	2±1	1±0	1±1
Microfibril-associated glycoprotein 4	MFAP4_HUMAN	1±1	1±1	1±1	2±1	1±1
Nidogen-1	NID1_HUMAN	1±1	2±1	17±11	5±5	4±3
Periostin	POSTN_HUMAN	6±8	6±5	**34±9*** **	15±11	**20±2*** **
RPE-spondin	RPESP_HUMAN	3±3	2±1	2±2	2±1	2±2
Secreted frizzled-related protein 3	SFRP3_HUMAN	4±5	2±3	2±2	2±1	1±1
Serum amyloid P-component	SAMP_HUMAN	23±10	46±28	19±7	**43±11*** **	29±6
SPARC	SPARC_HUMAN	6±9	1±1	1±1	6±9	2±2
Target of Nesh-SH3	TARSH_HUMAN	122 ±10	27±19	**58±48** **	**59±16*** **	**49±27*** **
Tenascin (Tenascin-C)[#]	TENA_HUMAN	46±39	82±37	**186±81*** **	81±8	84±48
Tenascin-X	TENX_HUMAN	55±52	27±6	**253±74*** **	245±198	99±38
Tetranectin	TETN_HUMAN	27±12	18±6	**12±4*** **	20±3	**15±8*** **
Thrombospondin-1	TSP1_HUMAN	19±13	7±4	10±4	11±4	11±5
Tubulointerstitial nephritis antigen like	TINAL_HUMAN	6±4	5±4	3±3	7±6	7±8
Vitronectin	VTNC_HUMAN	6±6	5±4	4±2	4±4	4±4
Collagens (14)						
Collagen α-1(I)[#]	CO1A1_HUMAN	29±14	48±40	**148±163*** **	**6±4*** **	**14±2*** **
Collagen α-1 (III)[#]	CO3A1_HUMAN	4±4	12±17	**60±78*** **	6±5	**18±13*** **
Collagen α-1 (IV)[#]	CO4A1_HUMAN	0±1	0±0	**37±24*** **	**70±52*** **	7±8
Collagen α-1 (VI)	CO6A1_HUMAN	44±37	38±32	104±81	80±46	49±34
Collagen α-1(XII)	COCA1_HUMAN	10±11	13±13	**68±15*** **	18±19	16±4
Collagen α-1(XIV)	COEA1_HUMAN	79±80	66±58	141±25	91±89	67±13
Collagen α-1(XV)	COFA1_HUMAN	22±15	18±9	**62±5*** **	**50±11*** **	**43±7*** **
Collagen α-1 (XVI)	COGA1_HUMAN	0±1	1±1	1±1	3±4	1±1
Collagen α-1(XVIII) [#]	COIA1_HUMAN	75±45	79±22	**171±19*** **	**164±61*** **	87±10
Collagen α-1(XXVIII)	COSA1_HUMAN	1±1	0±1	1±1	2±1	1±1
Collagen α-2(I)[#]	CO1A2_HUMAN	10±4	26±29	**78±83*** **	**3±4***	11±10
Collagen α-2(IV)[#]	CO4A2_HUMAN	10±5	3±1	**53±40*** **	**84±32*** **	21±16
Collagen α-2(VI)	CO6A2_HUMAN	15±13	8±6	36±27	27±4	12±11
Collagen α-3(VI)	CO6A3_HUMAN	118±94	102±50	**478±5*** **	**180±82*** **	**241±132*** **
Non-glycosylated ECM proteins (5)						
Annexin A2	ANXA2_HUMAN	32±29	124±80	45±46	36±30	36±37
Dermatopontin	DERM_HUMAN	12±15	10±10	5±6	10±14	7±9
Galectin-1	LEG1_HUMAN	16±11	18±4	**4±2*** **	17±16	16±9
TGF β-1-induced transcript 1 protein	TGFI1_HUMAN	4±3	1±0	3±2	3±5	10±9
TGF β-induced protein ig-h3	BGH3_HUMAN	13±10	12±10	25±12	14±12	20±15

DOI: 10.1161/CIRCGENETICS.112.964452

Other ECM-associated proteins (19)						
Apolipoprotein A-I[#]	APOA1_HUMAN	57±21	55±10	**28±20*****	**36±12***	45±15
Apolipoprotein A-I-binding protein	AIBP_HUMAN	2±3	2±1	2±2	3±3	4±2
Apolipoprotein A-IV	APOA4_HUMAN	9±14	7±10	1±0	3±4	3±4
Apolipoprotein B-100	APOB_HUMAN	1±2	4±5	1±2	1±1	3±3
Apolipoprotein D	APOD_HUMAN	12±9	3±4	6±2	11±4	7±3
Apolipoprotein E	APOE_HUMAN	3±2	1±1	1±0	1±0	1±1
Apolipoprotein H	APOH_HUMAN	12±4	12±5	17±9	20±8	13±7
Cysteine-rich protein 2	CRIP2_HUMAN	12±11	5±4	2±1	2±1	16±20
Extracellular superoxide dismutase [Cu-Zn]	SODE_HUMAN	78±32	51±17	61±23	66±9	77±7
Hepatoma-derived growth factor	HDGF_HUMAN	4±5	3±3	2±2	5±7	2±1
IGF-binding protein 7	IBP7_HUMAN	35±20	9±8	38±10	33±3	38±9
IGF-binding protein complex acid labile chain	ALS_HUMAN	1±1	3±2	1±0	2±1	2±1
LIM and cysteine-rich domains protein 1	LMCD1_HUMAN	1±1	1±0	1±0	1±0	1±0
Myeloperoxidase	PERM_HUMAN	1±0	1±1	2±1	1±1	1±0
Pigment epithelium-derived factor	PEDF_HUMAN	32±16	21±1	22±6	24±6	25±18
Protein-glutamine γ -glutamyltransferase 2	TGM2_HUMAN	10±16	10±16	21±15	21±33	19±30
Protein S100-A8	S10A8_HUMAN	7±4	25±41	7±11	9±14	2±2
Protein S100-A9	S10A9_HUMAN	5±4	19±29	1±0	1±1	1±1
Secreted phosphoprotein 24	SPP24_HUMAN	1±0	2±1	1±0	1±0	1±0
Proteases & protease inhibitors (12)						
Alpha-1-antitrypsin	A1AT_HUMAN	70±61	49±50	43±23	49±28	62±31
Calreticulin	CALR_HUMAN	9±14	10±9	10±16	15±23	13±20
Cathepsin B	CATB_HUMAN	1±0	2±2	1±0	1±0	1±0
Cathepsin D	CATD_HUMAN	13±22	3±3	5±8	10±16	7±11
Cathepsin Z	CATZ_HUMAN	5±7	2±2	4 ±4	9 ±14	5±6
Kallistatin	KAIN_HUMAN	2±2	2±1	3 ±1	2 ± 3	2±2
Leukocyte elastase inhibitor	ILEU_HUMAN	12±6	12±7	9 ±3	6 ± 2	8±3
Mast cell carboxypeptidase A	CBPA3_HUMAN	1±1	1±0	1±0	3±4	1±1
Metalloproteinase inhibitor 1	TIMP1_HUMAN	0±1	1±0	4±1	20±10	3±2
Plasmaglutamate carboxy-peptidase	PGCP_HUMAN	6±3	4±4	5±7	9±12	3±3
Procollagen C endo-peptidase enhancer 1	PCOC1_HUMAN	12±10	5±4	10±11	11±8	6±4
Tryptase alpha-1	TRYA1_HUMAN	6±3	2±2	2±3	7±4	6±2

List of all ECM proteins, ECM-related proteins and collagens identified by proteomics. Values are the number of assigned spectra and are means ± SD from three biological replicates. Bold font indicates significant differences versus control (-EDTA). Statistical analyses were performed using the *Qspec* method described in Choi *et al.* The Bayes Factors (BR) were *** FDR≤0.001 and BF>10, ** FDR≤0.01 and BF>8, * FDR≤0.05 and BF>6. [#], denotes proteins that are known MMP substrates, for references see online-only Data **Supplemental Table 2**

DOI: 10.1161/CIRCGENETICS.112.964452

Figure Legends:

Figure 1. Effect of exogenous MMPs. ECM and ECM-related proteins released from human radial arteries were analysed by LC-MS/MS. The log(fold change) for each of the differentially released proteins upon digestion with MMPs is illustrated. The proteins are ordered from the smallest to largest False Discovery Rate (FDR) with significant differential expression set at a FDR<5%. The differential release and corresponding FDR was calculated using the *Qspec* method, which utilises a model based on a hierarchical Bayes estimation of generalized linear mixed effects model (GLMM). The FDR, as per the *Qspec* method, was calculated using the Bayes Factors and a mixture model-based method of controlling the local FDR. The Bayes Factors (BR) were *** FDR≤0.001 and BF>10, ** FDR≤0.01 and BF>8, * FDR≤0.05 and BF>6. All protein identifications for ECM and ECM-related proteins are listed in **Table 1**.

Figure 2. Validation by immunoblotting. The conditioned media analysed by immunoblotting for fibronectin **(A)**, galectin-1 **(B)**, tenascin-C **(C)**, periostin **(D)** and tensacin-X **(E)**.

Figure 3. Spectral evidence for fragmentation. The color-coded heat map demonstrates the number of identified spectra for the 7 extracellular proteins in control and MMP samples and their molecular weight distribution after SDS-PAGE. 16 gel slices per lane were analysed by LC-MS/MS. Quantitative heat maps visualizing the characteristic laddering as blue to red color gradient were produced using the GenePattern software (version 3.2.3). CON, control arteries incubated MMP buffer.

Figure 4. Dose-dependency and specificity for MMPs. Immunoblotting for fibronectin, tenascin-C, periostin and tensacin-X after overnight incubation with 100 ng MMP/mg tissue (H), 20 ng MMP/mg tissue (L), or buffer only (Control = CON) **(A)**. Radial samples were incubated in plain reaction buffer (CON), with 100 ng/mg tissue MMP-3, -9 or -14 with (+) or without (-) the addition of 25 mM EDTA to inhibit MMP activity **(B)**.

Figure 5. Digestion of recombinant / purified proteins. Direct evidence for degradation by MMPs was provided by using recombinant / purified proteins: fibronectin **(A)**, tenascin-C **(B)** and periostin **(C)** were incubated with MMP-3, -9 and -14, separated by SDS-PAGE and stained in a 0.05% w/v Coomasie G-250, 5% v/v glacial acetic acid solution to monitor substrate degradation.

Figure 6. Potential cleavage sites for MMP-3, -9 and -14. The Venn diagram summarizes ECM and ECM-related proteins with non-tryptic peptides observed by LC-MS/MS. All non-tryptic peptides identified are listed in the online-only Data **Supplemental Table 3**. * indicates potential new MMP substrate, ** denotes new candidate substrates for this particular MMP.

Figure 7. Comparison to endogenous MMP-9 levels. HE-staining of a representative human thoracic aorta. I, intima; M, media **(A)**. MMP-9 levels in the NaCl extracts of four human aortic samples as detected by gelatinolytic zymography **(B)**. *New candidates substrates identified with exogenous MMP-9 **(C)**. Heat map visualizing their fragmentation with increasing endogenous MMP-9 expression **(D)**. Confirmation of cleavage of collagen VI upon digestion with MMP-9 **(E)**.

Figure 1

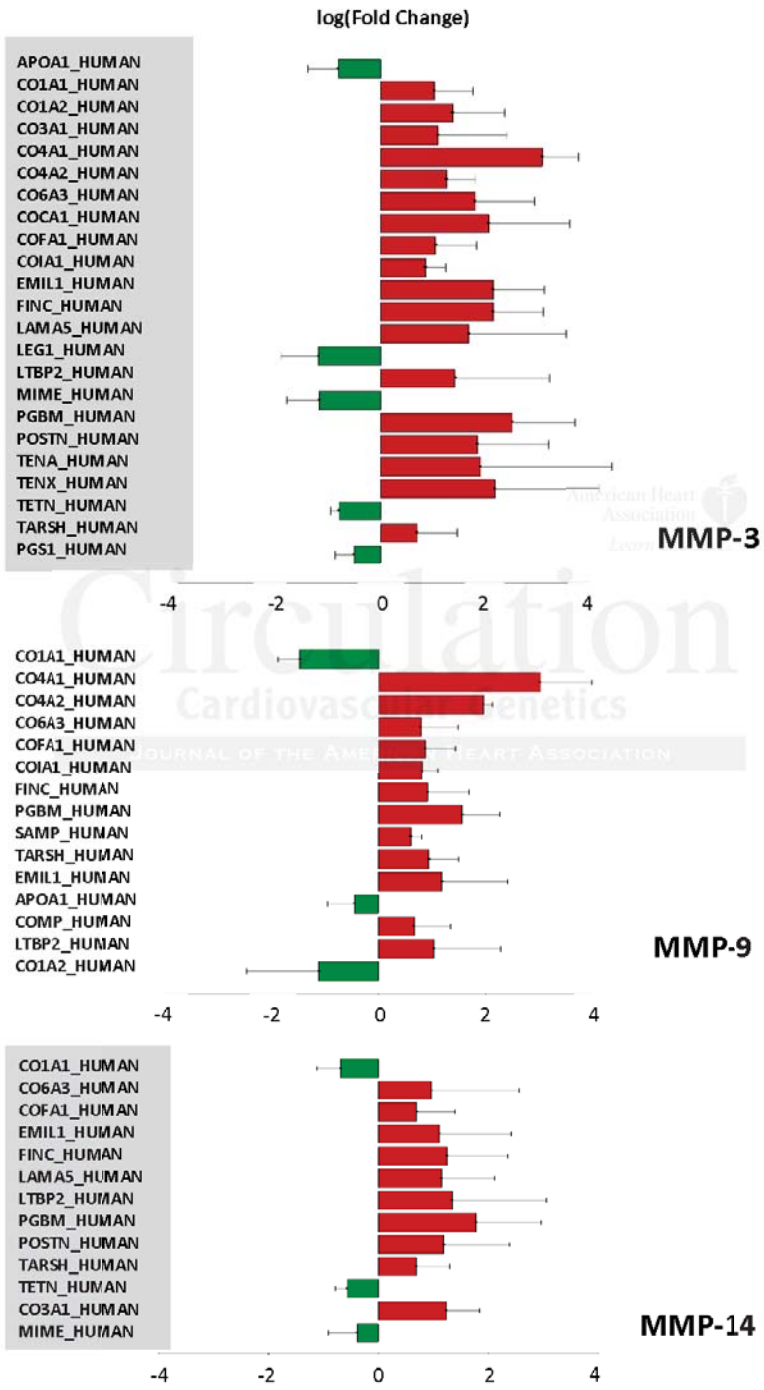
log(Fold Change)
APOA1_HUMAN
CO1A1_HUMAN
CO1A2_HUMAN
CO3A1_HUMAN
CO4A1_HUMAN
CO4A2_HUMAN
CO6A3_HUMAN
COCA1_HUMAN
COFA1_HUMAN
COIA1_HUMAN
EMIL1_HUMAN
FINC_HUMAN
LAMA5_HUMAN
LEG1_HUMAN
LTBP2_HUMAN
MIME_HUMAN
PGBM_HUMAN
POSTN_HUMAN
TENA_HUMAN
TENX_HUMAN
TETN_HUMAN
TARSH_HUMAN
PGS1_HUMAN
-4
-2
0
2
4
MMP-3
CO1A1_HUMAN
CO4A1_HUMAN
CO4A2_HUMAN
CO6A3_HUMAN
COFA1_HUMAN
COIA1_HUMAN
FINC_HUMAN
PGBM_HUMAN
SAMP_HUMAN
TARSH_HUMAN
EMIL1_HUMAN
APOA1_HUMAN
COMP_HUMAN
LTBP2_HUMAN
CO1A2_HUMAN
-4
-2
0
2
4
MMP-9
CO1A1_HUMAN
CO6A3_HUMAN
COFA1_HUMAN
EMIL1_HUMAN
FINC_HUMAN
LAMA5_HUMAN
LTBP2_HUMAN
PGBM_HUMAN
POSTN_HUMAN
TARSH_HUMAN
TETN_HUMAN
CO3A1_HUMAN
MIME_HUMAN
-4
-2
0
2
4
MMP-14

Figure 2

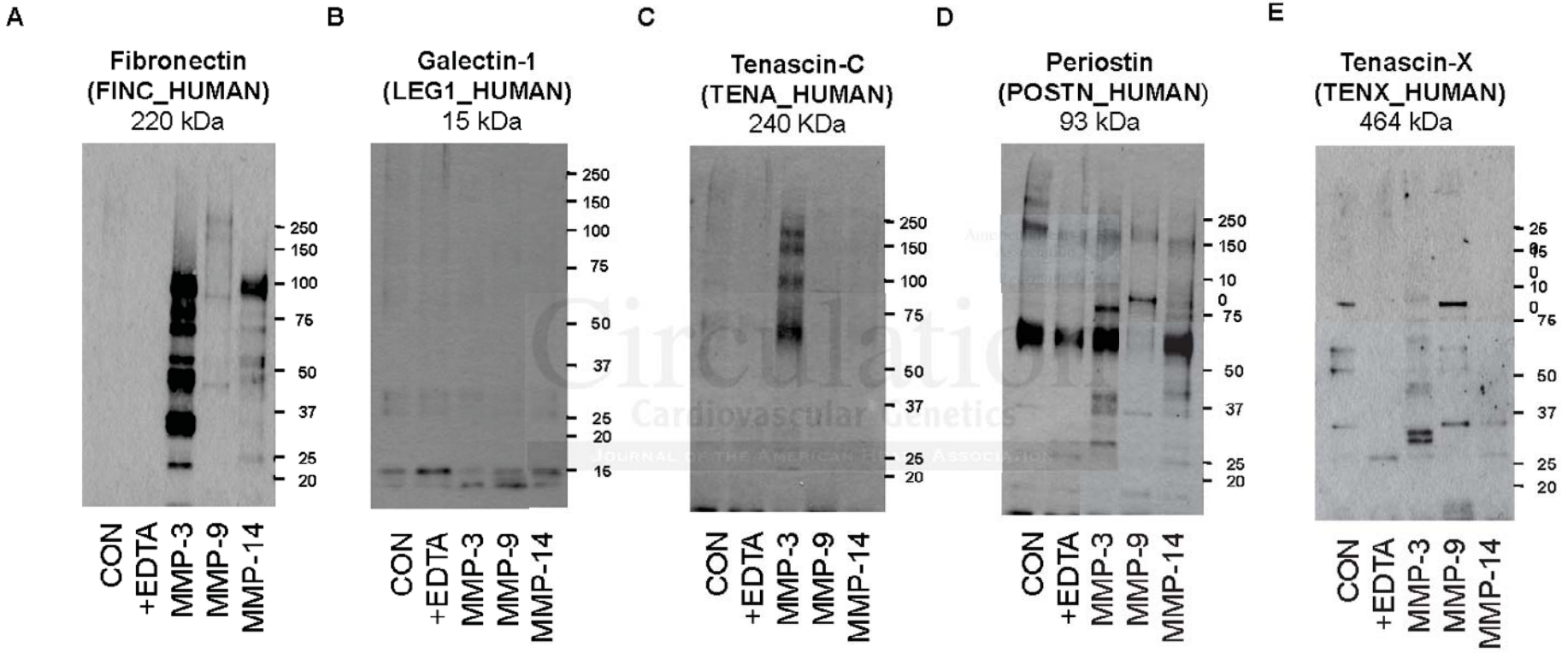
A
Fibronectin
(FINC_HUMAN)
220 kDa
250
150
100
75
50
37
25
20
CON
+EDTA
MMP-3
MMP-9
MMP-14
B
Galectin-1
(LEG1_HUMAN)
15 kDa
250
150
100
75
50
37
25
20
16
CON
+EDTA
MMP-3
MMP-9
MMP-14
C
Tenascin-C
(TENA_HUMAN)
240 KDa
250
150
100
75
50
37
25
20
CON
+EDTA
MMP-3
MMP-9
MMP-14
D
Periostin
(POSTN_HUMAN)
93 kDa
250
150
10
0
75
50
37
25
20
CON
+EDTA
MMP-3
MMP-9
MMP-14
E
Tenascin-X
(TENX_HUMAN)
464 kDa
25
0
10
0
75
50
37
25
20
CON
+EDTA
MMP-3
MMP-9
MMP-14

Figure 3

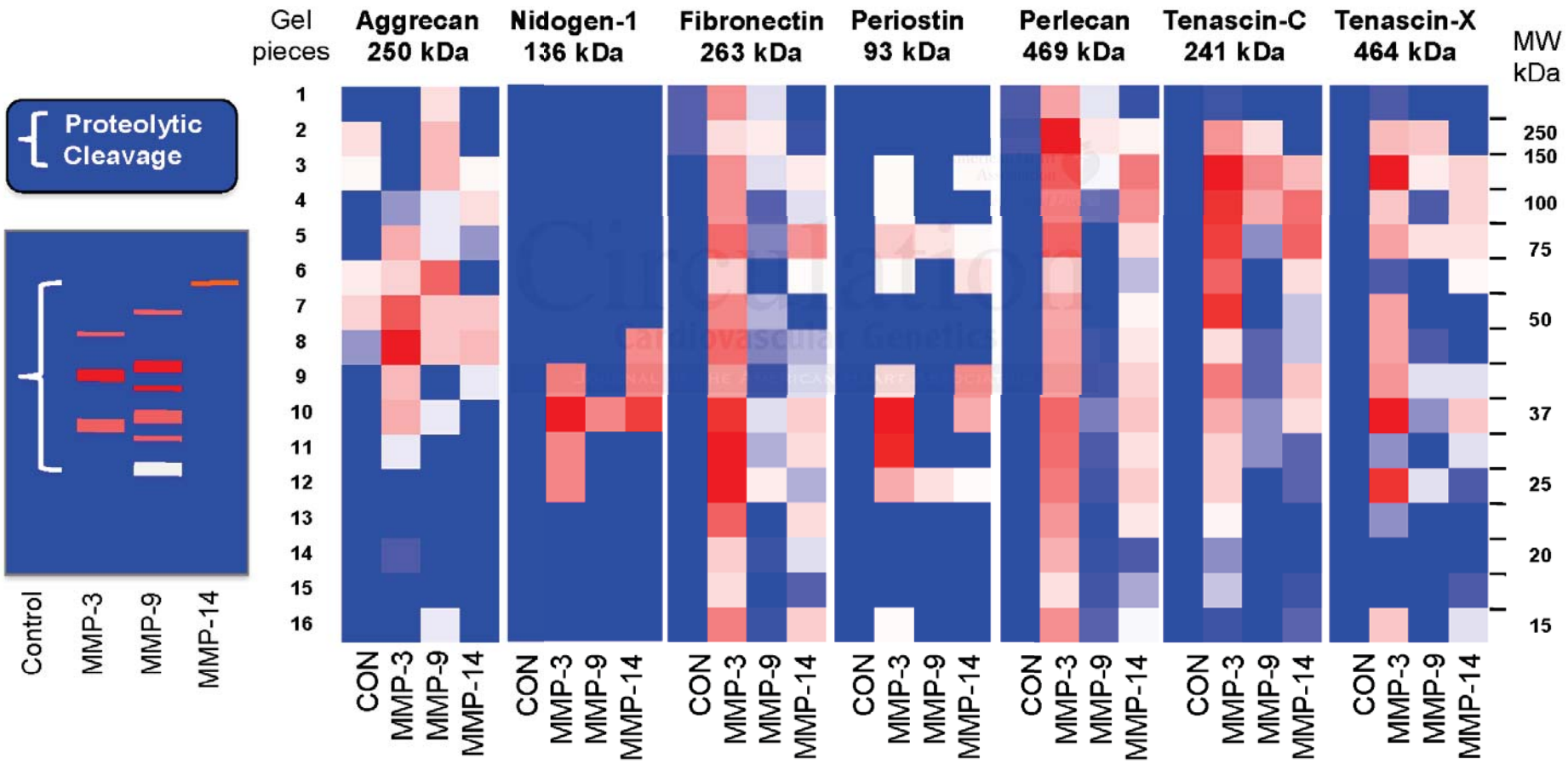
Proteolytic Cleavage
Control
MMP-3
MMP-9
MMP-14
Gel pieces
1
2
3
4
5
6
7
8
9
10
11
12
13
14
15
16
Aggrecan 250 kDa
Nidogen-1 136 kDa
Fibronectin 263 kDa
Periostin 93 kDa
Perlecan 469 kDa
Tenascin-C 241 kDa
Tenascin-X 464 kDa
CON
MMP-3
MMP-9
MMP-14
MW kDa
250
150
100
75
50
37
25
20
15

Figure 4

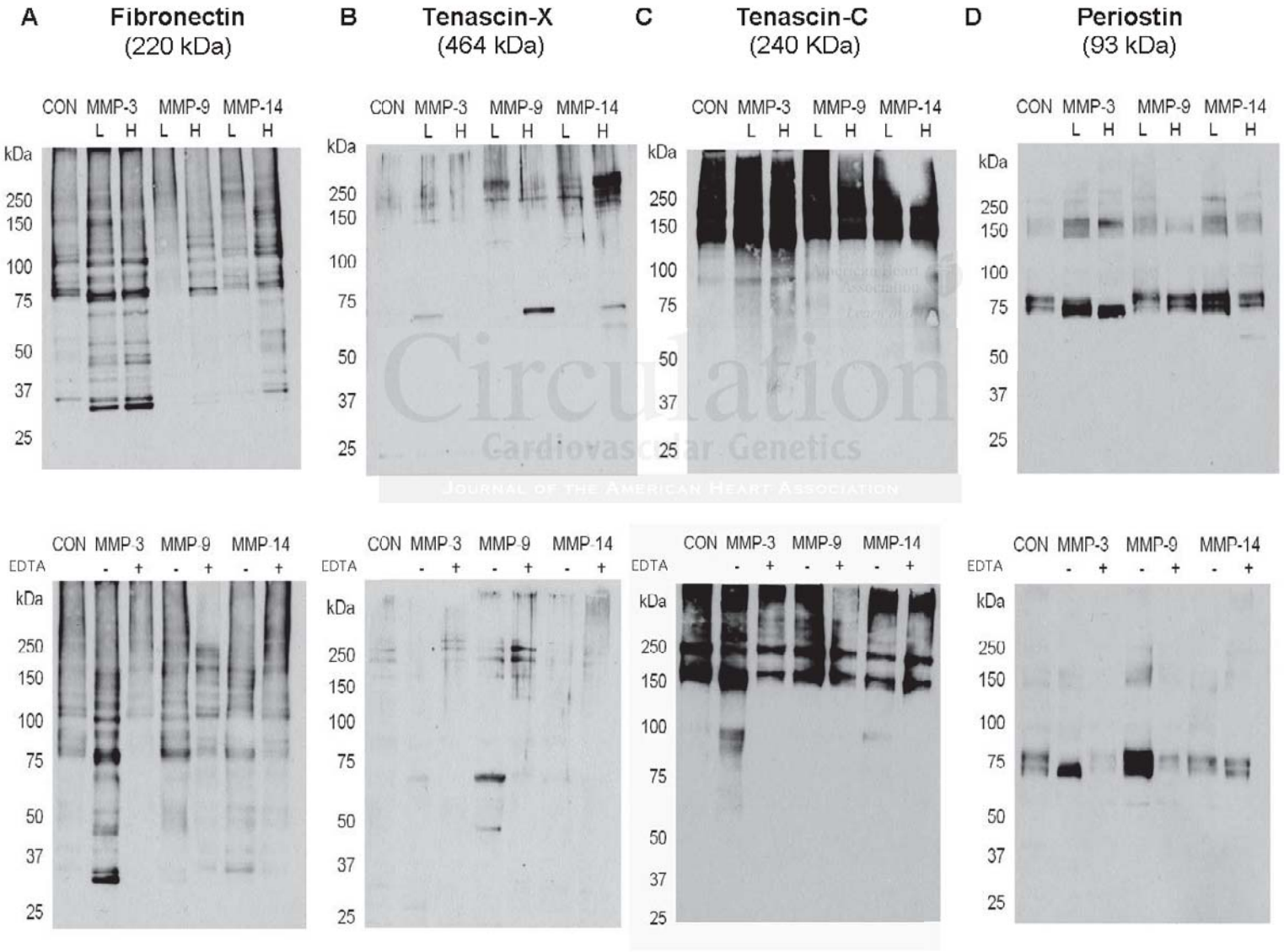
A
Fibronectin
(220 kDa)
B
Tenascin-X
(464 kDa)
C
Tenascin-C
(240 KDa)
D
Periostin
(93 kDa)
CON MMP-3 MMP-9 MMP-14
L H L H L H
kDa
250
150
100
75
50
37
25
EDTA
- + - + - +

Figure 5

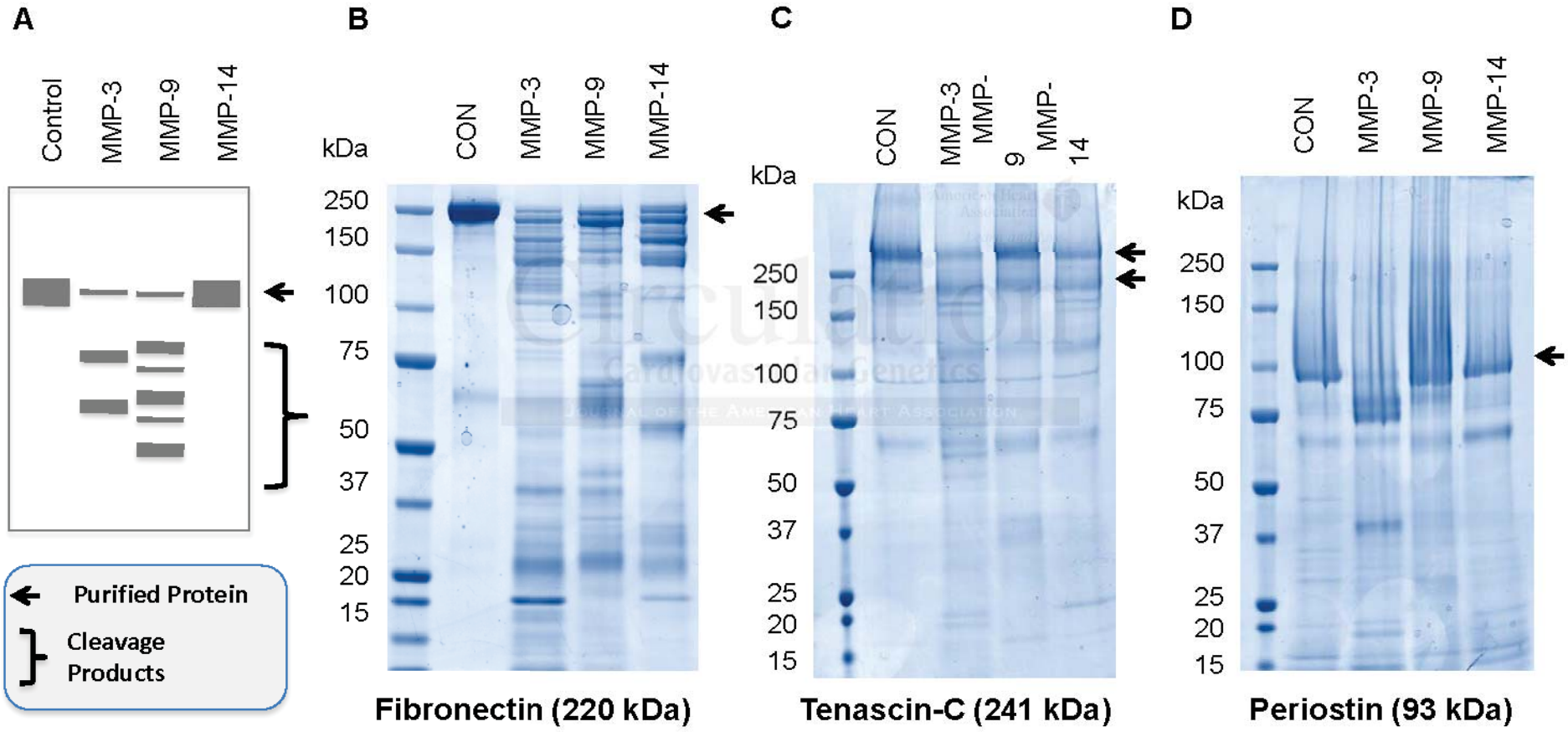
A
Control
MMP-3
MMP-9
MMP-14
Purified Protein
Cleavage Products
B
kDa
CON
MMP-3
MMP-9
MMP-14
250
150
100
75
50
37
25
20
15
Fibronectin (220 kDa)
C
kDa
CON
MMP-3
MMP-9
MMP-14
250
150
100
75
50
37
25
20
15
Tenascin-C (241 kDa)
D
kDa
CON
MMP-3
MMP-9
MMP-14
250
150
100
75
50
37
25
20
15
Periostin (93 kDa)

Figure 6

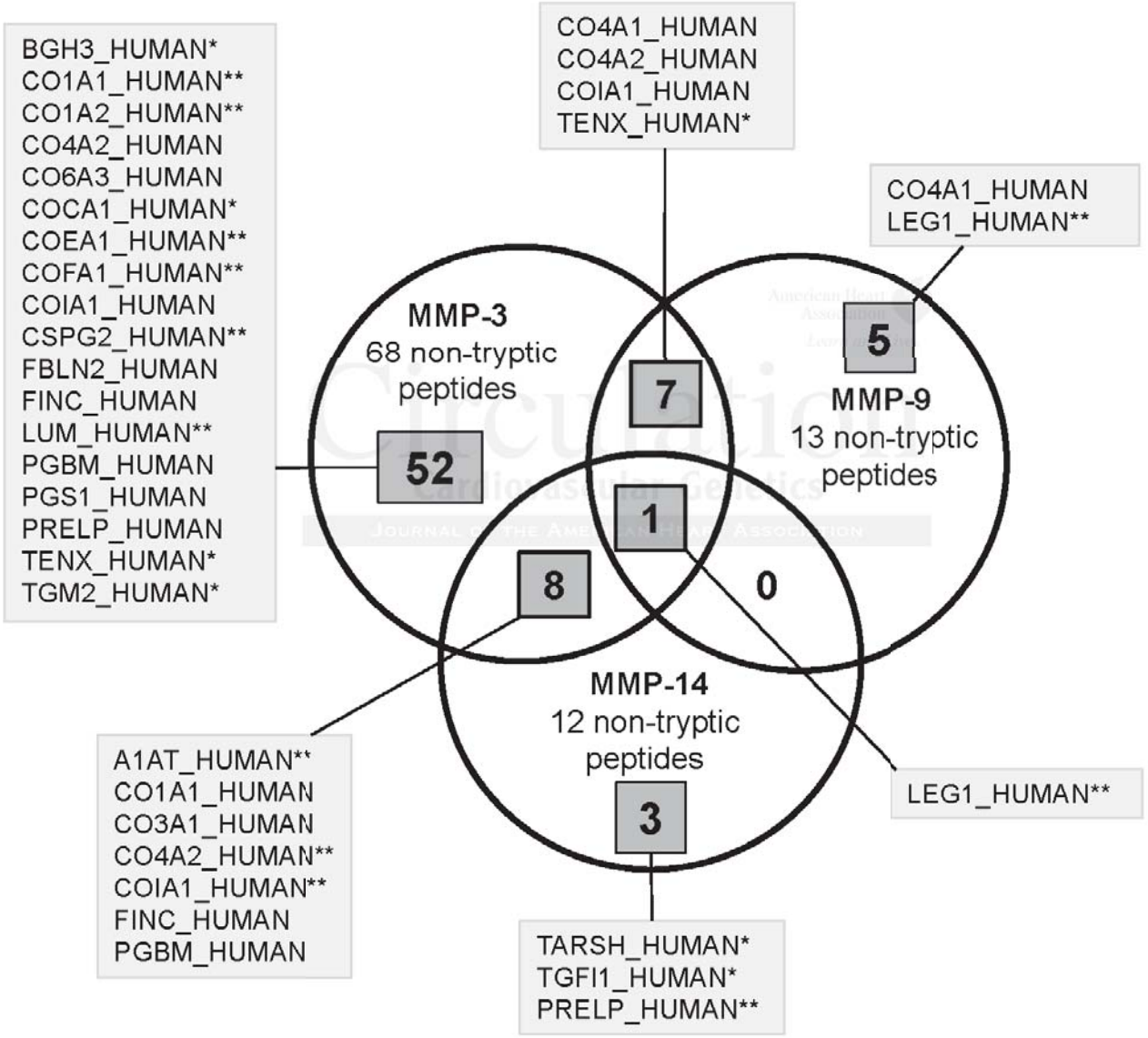
BGH3_HUMAN*
CO1A1_HUMAN**
CO1A2_HUMAN**
CO4A2_HUMAN
CO6A3_HUMAN
COCA1_HUMAN*
COEA1_HUMAN**
COFA1_HUMAN**
COIA1_HUMAN
CSPG2_HUMAN**
FBLN2_HUMAN
FINC_HUMAN
LUM_HUMAN**
PGBM_HUMAN
PGS1_HUMAN
PRELP_HUMAN
TENX_HUMAN*
TGM2_HUMAN*
CO4A1_HUMAN
CO4A2_HUMAN
COIA1_HUMAN
TENX_HUMAN*
CO4A1_HUMAN
LEG1_HUMAN**
MMP-3
68 non-tryptic
peptides
52
7
5
MMP-9
13 non-tryptic
peptides
1
8
0
MMP-14
12 non-tryptic
peptides
3
A1AT_HUMAN**
CO1A1_HUMAN
CO3A1_HUMAN
CO4A2_HUMAN**
COIA1_HUMAN**
FINC_HUMAN
PGBM_HUMAN
LEG1_HUMAN**
TARSH_HUMAN*
TGFI1_HUMAN*
PRELP_HUMAN**

Figure 7

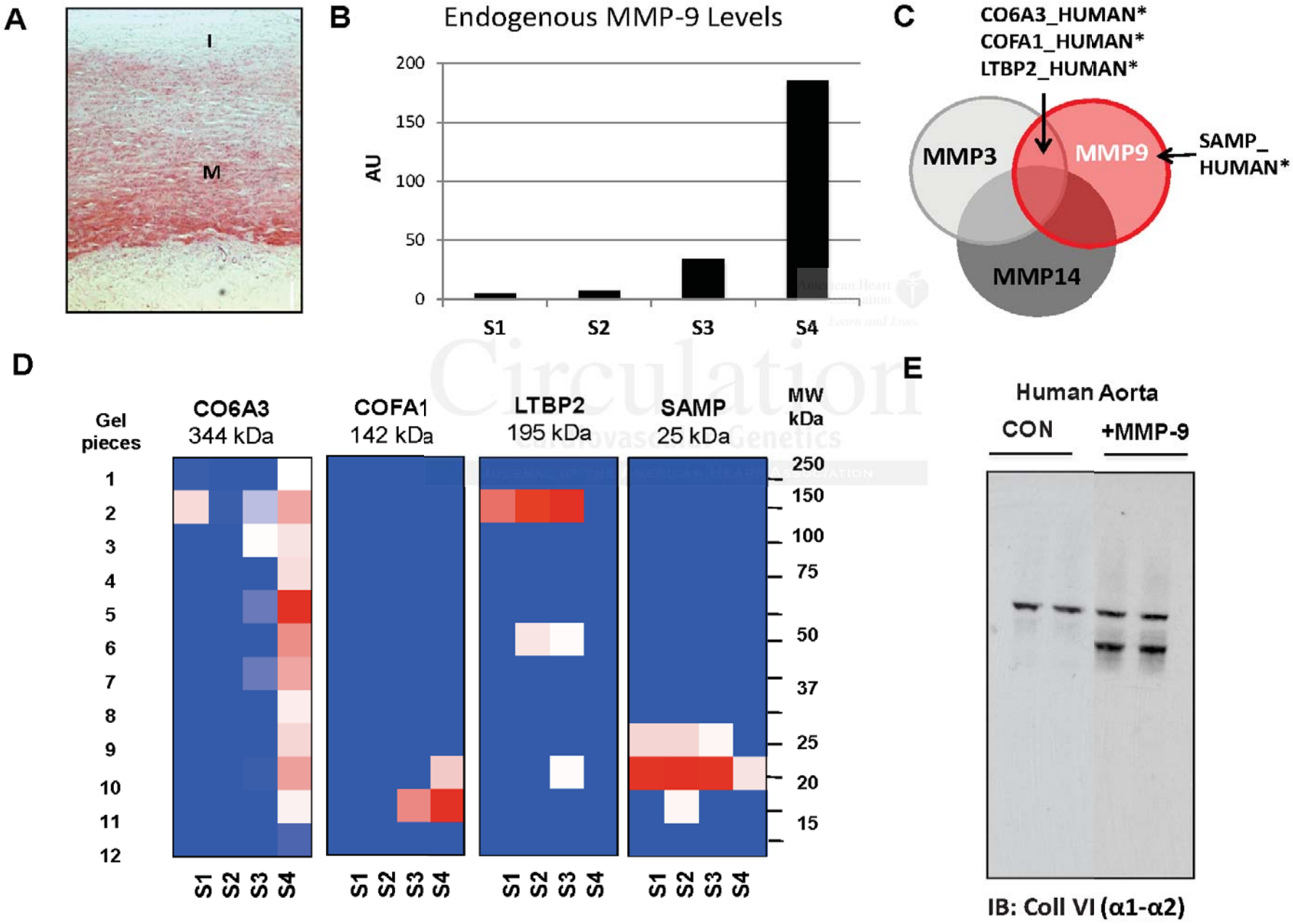
A
I
M
B
Endogenous MMP-9 Levels
AU
200
150
100
50
0
S1
S2
S3
S4
C
CO6A3_HUMAN*
COFA1_HUMAN*
LTBP2_HUMAN*
MMP3
MMP9
MMP14
SAMP_
HUMAN*
D
Gel pieces
CO6A3
344 kDa
COFA1
142 kDa
LTBP2
195 kDa
SAMP
25 kDa
MW kDa
250
150
100
75
50
37
25
20
15
1
2
3
4
5
6
7
8
9
10
11
12
S1 S2 S3 S4
E
Human Aorta
CON
+MMP-9
IB: Coll VI (α1-α2)